Narrow linewidth two-color polarization spectroscopy due to the atomic coherence effect in a ladder-type atomic system

Baodong Yang (杨保东)[1,2,*], Jinfang Zhang (张锦芳)[1], and Junmin Wang (王军民)[2]

[1]*College of Physics and Electronic Engineering, Shanxi University, Taiyuan 030006, China*

[2]*State Key Laboratory of Quantum Optics and Quantum Optics Devices and Institute of Opto-Electronics, Shanxi University, Taiyuan 030006, China*

**Corresponding author: ybd@sxu.edu.cn*

Received April 3, 2019; accepted May 17, 2019; posted online July 24, 2019

An experimental investigation of two-color polarization spectroscopy (TCPS) is presented based on the cesium $6S_{1/2}-6P_{3/2}-8S_{1/2}$ (852.3 nm + 794.6 nm) ladder-type system in a room-temperature vapor cell. The dependency of line shapes of TCPS on the power of a 852.3 nm pump and a 794.6 nm probe laser is measured in detail, and we confirm that the linewidth of TCPS in a counter-propagating configuration between the pump and probe laser beams is obviously narrower than that of a co-propagating configuration, due to the atomic coherence effect. It is helpful for laser stabilization of the excited state transition using TCPS without frequency modulation.

OCIS codes: 300.6210, 020.1670, 020.3690, 300.3700.

doi: 10.3788/COL201917.093001.

Excited state spectroscopy has been widely used in many applications, such as high-resolution spectroscopy, measurement of hyperfine structure constants of atoms[1–2], detection of Rydberg states[3], frequency stabilization[4–5], diamond-level four-wave mixing[6], and two-color laser cooling/trapping of neutral atoms[7–10]. A sophisticated technique for obtaining an excited state spectrum is the optical-optical double resonance (OODR) spectrum[11], but sometimes its spectral signal-to-noise ratio (SNR) is low in a large spontaneous emission rate atomic system due to difficultly in populating atoms into the intermediate excited state from the ground state. In 2004, the double-resonance optical pumping (DROP) technique was first demonstrated in a ladder-type atomic system[12], which dramatically improved the spectral SNR between the excited states transition. Its key idea is to detect the population change of the ground state from a stepwise two-photon optical pumping process[13]. When the DROP and OODR spectra as references are applied to the laser frequency stabilization, an extra frequency modulation signal is often imposed on the laser to obtain a frequency discriminating signal. Fortunately, a two-color polarization spectroscopy (TCPS) method for obtaining the Doppler-free excited state spectrum was reported by Carr *et al.* in experiment[14] and Noh in theory[15] based on the cesium (Cs) atom $6S_{1/2}-6P_{3/2}-7S_{1/2}$ ladder-type system, and we have applied the TCPS to the laser frequency offset locking by marrying the modulation sideband with a fiber-pigtailed waveguide-type electro-optical phase modulator[16]. Kulatunga *et al.* also experimentally investigated the dependency of the TCPS on the frequency detuning of a pump laser in the ^{87}Rb atoms $5S_{1/2}-5P_{3/2}-5D_{5/2}$ ladder-type system[17]. The TCPS provides a dispersive signal for the laser frequency stabilization of an excited-to-excited state transition without frequency modulation as in traditional polarization spectroscopy, which can further improve the frequency stabilization of the laser[18].

In this Letter, we experimentally investigate the TCPS based on the ^{133}Cs $6S_{1/2}-6P_{3/2}-8S_{1/2}$ ladder-type atomic system. Different from the previous work on the TCPS, which is only experimentally demonstrated in the counterpropagating (CTP) configuration between the pump and probe beams[14–17], here we also realize the TCPS in the co-propagating (CP) configuration. We further discover the influence of the electromagnetically induced transparency (EIT) atomic coherence on the linewidth of the TCPS by comparing the evolution of the TCPS line shapes for the CTP and CP configurations in the case of different pump and probe light powers.

The relevant energy levels of Cs atoms are shown in Fig. 1; the natural linewidths of excited states $6P_{3/2}$ and $8S_{1/2}$ are 5.2 MHz and 2.2 MHz, respectively. The frequency of the circularly polarized 852.3 nm pump laser is tuned to the $6S_{1/2}\,F=4-6P_{3/2}\,F'=5$ transition, and the pump beam passes through a room-temperature Cs vapor cell, so some atoms in the ground state $6S_{1/2}\,F=4$ are unevenly populated on the $6P_{3/2}\,F'=5$ Zeeman sublevels, inducing an anisotropy in the atomic medium. The frequency of the linearly polarized 794.6 nm probe laser is scanned over the excited state $6P_{3/2}\,F'=5-8S_{1/2}\,F''=4$ transition. The probe laser can be seen as the combination of σ^+ and σ^- circularly polarized components. From Fig. 1, we can see that the σ^- component is more preferentially absorbed by the anisotropy atomic medium than σ^+; furthermore, the propagation speed of the two components in the medium is also different, so these factors result in a change in polarization of the probe after leaving the Cs vapor cell. Then, using a half-wave plate and a

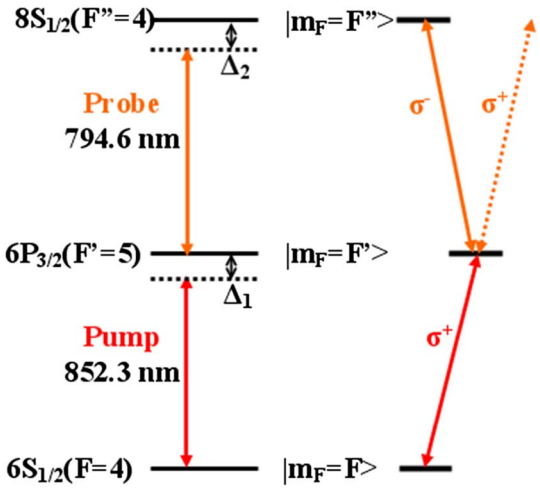

Fig. 1. Energy level diagram of Cs $6S_{1/2} - 6P_{3/2} - 8S_{1/2}$ for two-color polarization spectroscopy: the circularly polarized 852.3 nm pump laser drives σ^+ transitions and induces an anisotropy in the atomic medium, which is detected by a linearly polarized 794.6 nm probe laser between the excited state $6P_{3/2} - 8S_{1/2}$ transition.

polarizing beam splitting cube (PBS), the probe field is resolved into the two orthogonal linear components, which are detected by a balanced detector to obtain a dispersive signal as a so-called TCPS. Generally, the 852.3 nm pump laser is resonant on one of the hyperfine transitions between the ground state $6S_{1/2}$ and the intermediate state $6P_{3/2}$, so its frequency detuning $\Delta_1 = 0$. This TCPS signal is proportional to the dispersion described by[14]

$$\Delta n = \Delta\alpha_0 \frac{2c}{\omega_{32}\Gamma_3} \cdot \frac{\Delta_2}{1 + (2\Delta_2/\Gamma_3)^2}, \tag{1}$$

where Δn is the difference of the refractive indices and $\Delta\alpha_0$ is the maximum difference of the absorption coefficient for the σ^+ and σ^- components. Δ_2 is the frequency detuning of the probe laser, c is the speed of light in vacuum, $\Gamma_3 = 2.2$ MHz is the natural linewidth of the $8S_{1/2}$ state, and ω_{32} is the central frequency of $6P_{3/2}\,F' = 5 - 8S_{1/2}\,F'' = 4$ transition. Δn is a function of the frequency detuning Δ_2 of the 794.6 nm probe laser, and its line shape is a dispersion-like signal—the TCPS.

The schematic of the experimental setup for the TCPS is shown in Fig. 2. The 852.3 nm pump and the 794.6 nm probe laser beams are derived from the two separate external cavity diode lasers in a Littrow configuration, and their linewidth is estimated to be $<\sim$1 MHz. The frequency of the pump laser is locked on the $6S_{1/2}\,F = 4 - 6P_{3/2}\,F' = 5$ transition using the saturated absorption spectroscopy from the detector PD1, while the probe laser is scanned over the $6P_{3/2} - 8S_{1/2}$ transition. The pump and probe beams have a $1/e^2$ diameter $\sim$1.6 mm and $\sim$1.2 mm, respectively. The two beams are overlapped in the Cs cell 2 (25 mm in diameter, 50 mm in length) via dichroic filters (DFs) in the CTP or CP configuration by blocking beam1 or beam2 from the 852.3 nm laser. The TCPS is obtained in the balanced detector PD2. The frequency axis of the TCPS is calibrated by a confocal Fabrey–Perot cavity with a finesse of $\sim$200 and a free spectral range of $\sim$750 MHz not shown in Fig. 2. The TCPS is used as a frequency discriminating signal that is fed back to the piezoelectric transducer (PZT) port of the 794.6 nm laser by a proportional-integral-differential (PID) module for frequency locking.

Figure 3 is a typical TCPS signal corresponding to the excited state $6P_{3/2}\,F' = 5 - 8S_{1/2}\,F'' = 4$ hyperfine transition for the CP configuration; S_1 and S_2 are the respective signals from one photodiode of the balanced detector PD2. In order to facilitate the subsequent discussion, the magnitude, linewidth, and slope of the TCPS line shape are illustrated in Fig. 3.

Figure 4 shows the development of the magnitude, linewidth, and slope of the TCPS as functions of the 852.3 nm pump power at the fixed 794.6 nm probe power $\sim$0.20 mW for the CP and CTP configurations. As the pump power is

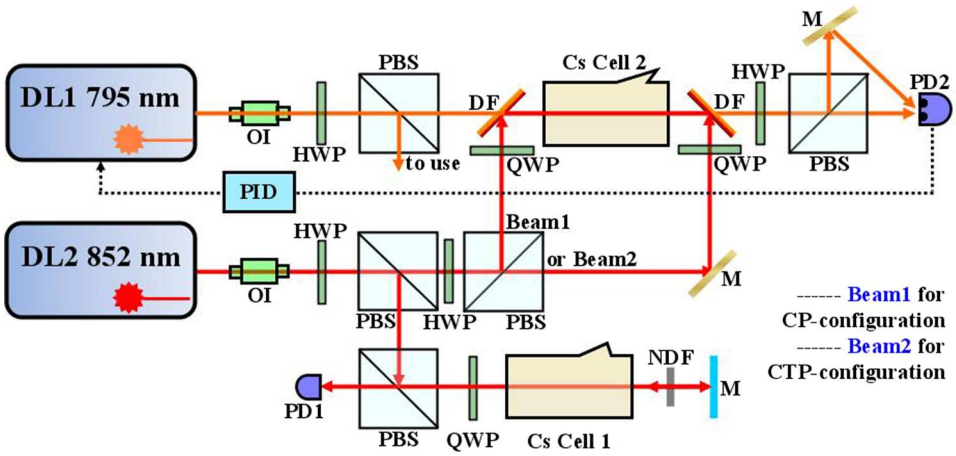

Fig. 2. Schematic diagram of the experimental setup for two-color polarization spectroscopy. DL: diode laser; OI: optical isolator; HWP: half-wave plate; QWP: quarter-wave plate; PBS: polarizing beam splitting cube; DF: dichroic filter; M: mirror; NDF: neutral density filter; PD: photodiode detector; Cs cell: cesium vapor cell.

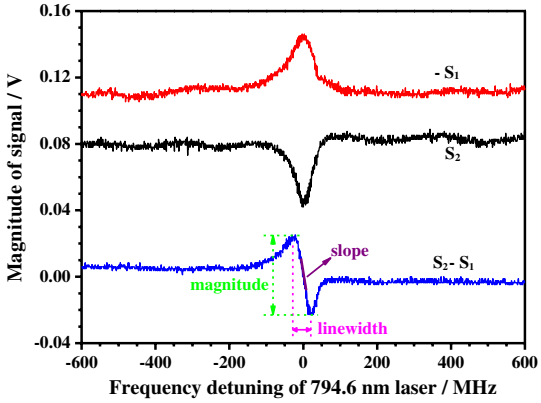

Fig. 3. Typical TCPS corresponding to the excited states $6P_{3/2}\,F'=5-8S_{1/2}\,F''=4$ hyperfine transition for the co-propagating configuration.

increased, the magnitude of the TCPS rapidly increases when the pump power <~1.0 mW, and then reaches a saturation level. From Fig. 4(a), it is clearly seen that the magnitude of the TCPS for the CTP configuration is about three times as big as that for the CP configuration. The linewidth of the TCPS also increases with the increasing pump power, but the linewidth of the TCPS for the CTP configuration is obviously narrower than that for the CP configuration, as shown in Fig. 4(b). When the power of the pump laser is changed from ~0.05 mW to ~5.5 mW, the linewidth of the TCPS is only increased from ~5.8 MHz to ~27.2 MHz for the CTP configuration, while it is increased from ~9.3 MHz to 66.2 MHz for the CP configuration. This is mainly because there exists an atomic coherence effect such as EIT (here, the 852.3 nm laser working on the lower transition is the probe laser, and the 794.6 nm laser operating on the upper transition is the coupling laser, which are contrary to the definition of TCPS indicated by Fig. 1) only for the CTP configuration in a ladder-type atomic system, as indicated by Fig. 5, which suppresses the linewidth of the TCPS. Specifically, in a ladder-type EIT atomic system, the complex susceptibility using standard semiclassical methods under the weak 852.3 nm probe laser approximation is $\chi=\chi'+i\chi''$, and the real part χ' and imaginary part χ'' are related to the dispersion and absorption of the atomic medium, respectively[19,20], as follows:

$$\chi(v)\,dv=\frac{4i\,g_{21}^2/\varepsilon_0}{\gamma_{21}-i\Delta_1-i\frac{\omega_1}{c}v+\frac{\Omega_2^2/4}{\gamma_{31}-i(\Delta_1+\Delta_2)-i(\omega_1\pm\omega_2)v/c}}N(v)\,dv,$$
$$N(v)=\frac{N}{u\sqrt{\pi}}\,e^{-v^2/u^2}\quad\text{and}\quad u=\sqrt{2kT/m}. \tag{2}$$

Here, ω_{21} is the frequency of Cs $6S_{1/2}\,F=4-6P_{3/2}\,F'=5$ transition, ω_1 is the frequency of the 852.3 nm laser, and so its frequency detuning $\Delta_1=\omega_1-\omega_{21}$. Similarly, ω_{32} is the frequency of the $6P_{3/2}\,F'=5-8S_{1/2}\,F''=4$ transition, ω_2 is the frequency of the 794.6 nm laser, and $\Delta_2=\omega_2-\omega_{32}$. g_{21} is the dipole moment matrix element for the $6S_{1/2}\,F=4-6P_{3/2}\,F'=5$ transition, and Ω_2 is the Rabi frequency of the 794.6 nm laser. If collisional dephasing is negligible, the decay rates are given by $\gamma_{ij}=(\Gamma_i+\Gamma_j)/2$, where $\Gamma_{i(j)}$ is the natural decay rate of level $i(j)$. N is the density of Cs atoms in the vapor cell, v is the speed of Cs atoms, u is the most probable velocity, k is the Boltzmann constant, T is the temperature, and m is the mass of a Cs atom.

In Eq. (2), the term $-i(\omega_1+\omega_2)v/c$ corresponds to the CP configuration, while the term $-i(\omega_1-\omega_2)v/c$ corresponds to the CTP configuration. According to

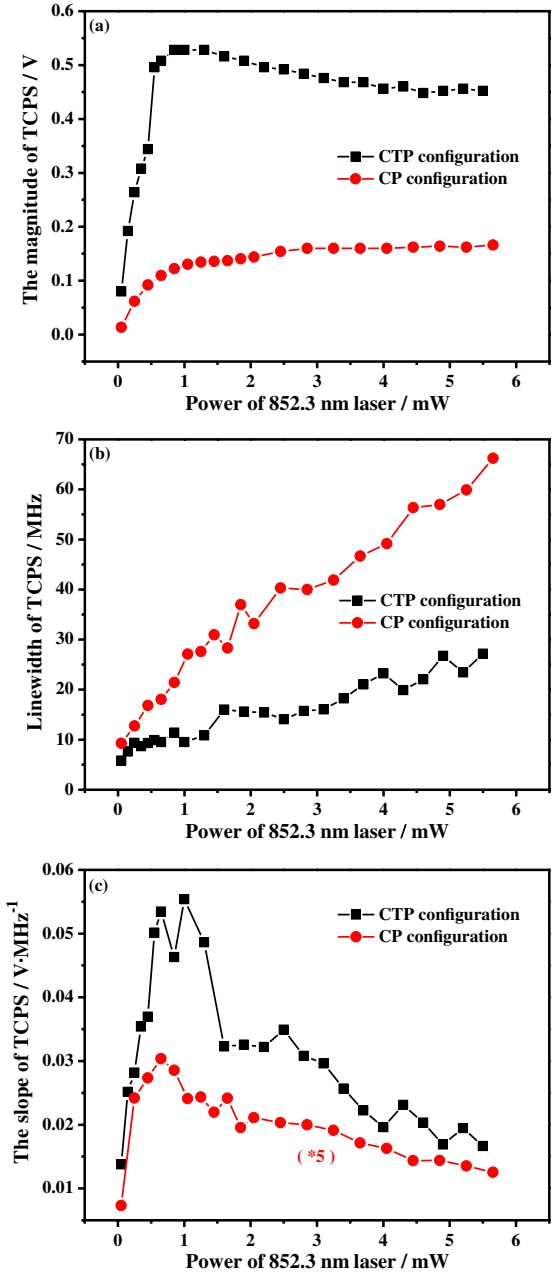

Fig. 4. Evolution of the (a) magnitude, (b) linewidth, and (c) slope of two-color polarization spectra with increasing 852.3 nm pump power for the counterpropagating and co-propagating experimental configurations between the pump and probe laser beams.

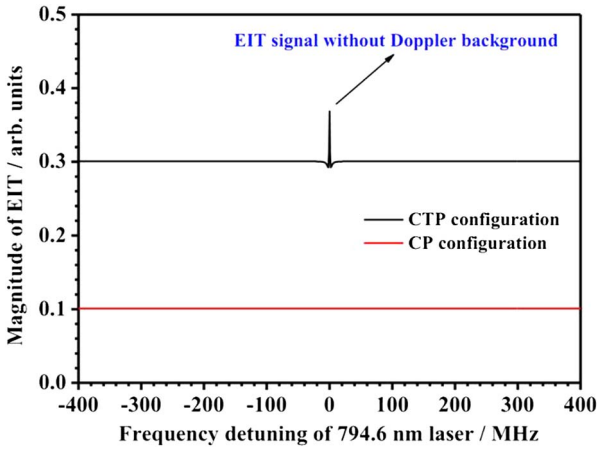

Fig. 5. In the TCPS scanning mode, a theoretical comparison of the EIT atomic coherence effect between the counterpropagating and co-propagating experimental configurations between the pump and probe laser beams in a ladder-type atomic system.

Eq. (2), the calculated transmittance spectra of the 852.3 nm laser field for the EIT in the TCPS scanning mode (the frequency of the 852.3 nm laser is locked, while the 794.6 nm laser is scanned) are shown in Fig. 5. For the CTP configuration, an obvious EIT peak without the Doppler background can be obtained due to the two-photon coherence; however, for the CP configuration, almost no signal is observed in a flat spectral background[20].

To further clarify the influence of the atomic coherence EIT component on the linewidth of the TCPS in the experiment, the power of the 852.3 nm and 794.6 nm lasers is set to ~0.23 mW in the Cs vapor cell 2, the 852.3 nm laser beam is set as a circularly polarized light, and the 794.6 nm laser beam is a linearly polarized light. In the same experimental conditions, the TCPS (the 794.6 nm laser as the probe field is detected by PD2 in Fig. 2) and EIT/DROP (the beam1 or beam2 from the 852.3 nm laser is the probe field, and its corresponding PD is not shown in Fig. 2) are simultaneously recorded for the CTP and CP configurations, respectively, as shown in Fig. 6. The

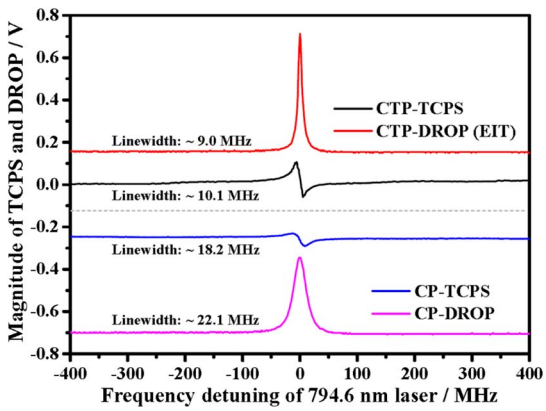

Fig. 6. Experimental comparison of TCPS and DROP/EIT between the counterpropagating and co-propagating experimental configurations between the pump and probe laser beams.

DROP spectrum is based on a two-photon optical pumping process in a five energy-level atomic model, it exists in the CTP and CP configurations[12], but the EIT effect merely exists in the CTP configuration in a ladder-type atomic system[19–21], as indicated by Fig. 5, which is an atomic coherence process. So for the CTP experimental configuration, the DROP and EIT effects all make contributions to the transmission spectrum of the 852.3 laser field with the linewidth ~9.0 MHz. Especially for the weak 852.3 nm laser field, the DROP contribution will be largely reduced, and the transmission spectra will have a highly pure EIT peak with a more narrow spectral linewidth, as seen in Fig. 5. However, for the CP experimental configuration, the transmission spectrum of the 852.3 laser field with the linewidth ~22.1 MHz mainly stems from the contribution of the DROP component because the DROP effect is not an atomic coherence process; thus, the spectral linewidth is obviously broad in comparison with the DROP/EIT spectrum of the CTP configuration. We know that the major differences between the DROP/EIT and TCPS techniques are their detection means. The DROP/EIT spectrum is a direct detection of the 852.3 nm laser beam, and the TCPS spectrum is a differential detection of the 794.6 nm laser beam, as shown in Fig. 2, but they all correspond to the same hyperfine transition line between the excited states $6P_{3/2}\,F' = 5 - 8S_{1/2}\,F'' = 4$. For the Cs atoms in vapor cell 2, they feel the same laser fields for the DROP/EIT and the TCPS spectra. So different detection means only result in different spectral line shapes (a dispersion-like signal for the TCPS, a peak signal for the DROP/EIT), and do not change the interaction between the Cs atoms and the two laser fields. Thus, the TCPS and DROP/EIT have an approximately equivalent spectral linewidth for the CTP or CP configuration, as shown in Fig. 6. So it is confirmed that the linewidth of the TCPS for the CTP configuration is narrower than that for the CP configuration, mainly due to the EIT atomic coherence effect.

The above changes in magnitude and linewidth of the TCPS in Fig. 4 lead to the fact that the slope (that is, the ratio of the magnitude to linewidth of the TCPS) of the TCPS presents an earlier increase and later decrease trend for the CTP and CP configurations, as seen in Fig. 4(c). In addition, the slope of the TCPS for the CTP configuration is near one order higher than that for the CP configuration at the pump power ~1.0 mW, which is greatly helpful for the frequency stabilization of 794.6 nm probe laser.

Figure 7 shows the evolution of the line shapes of the TCPS with the power of the 794.6 nm probe beam at the fixed 852.3 nm pump power ~0.20 mW. Different from Fig. 4(a), the magnitude of the TCPS is increasing monotonously for the growing power of the probe laser. With the increase of probe power, the linewidth of the TCPS grows very slowly in comparison with the experimental results for the changing pump power, as shown in Figs. 4(b) and 7(b). This significant difference results from the following reasons: for a ladder-type atomic

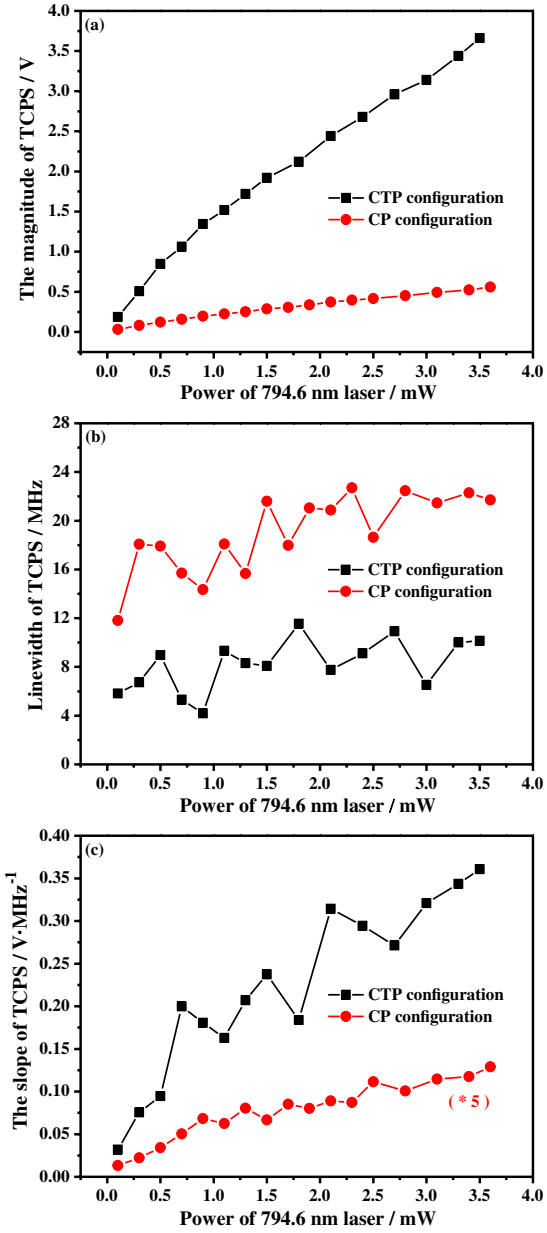

Fig. 7. Evolution of the (a) magnitude, (b) linewidth, and (c) slope of two-color polarization spectra with increasing 794.6 nm probe power for the counterpropagating and copropagating experimental configurations between the pump and probe laser beams.

system, the EIT atomic coherence effect will be enhanced with the increasing power of the 794.6 nm laser operating on the upper transition, which remarkably suppresses the linewidth of the TCPS [~4.2 MHz–~10.9 MHz for the CTP configuration, as shown in Fig. 7(b)]; however, this coherence effect will be destroyed via the spontaneous decay with the growing power of the 852.3 nm laser working on the lower transition. So when the power of the 852.3 nm laser is becoming big, the linewidth of the TCPS is obviously broadened from ~5.8 MHz to ~27.2 MHz for the CTP configuration seen in Fig. 4(b), and will be evolved into Autler–Townes splitting for the stronger 852.3 nm laser[14]. The above changes of magnitude and linewidth of the TCPS lead to a monotonous rise of the slope of the TCPS with the increasing power of 794.6 nm probe field, as shown in Fig. 7(c).

In conclusion, we present an investigation of the TCPS based on the Cs $6S_{1/2} - 6P_{3/2} - 8S_{1/2}$ (852.3 nm + 794.6 nm) atomic system in a room-temperature vapor cell. The evolution of the TCPS line shapes with increasing power of the pump and probe beams is measured, and is compared between the CP and CTP configurations. The experimental results and theoretical analysis have proved that the ladder-type EIT atomic coherence effect suppresses the linewidth of atomic excited spectra for the CTP configuration, which results in the linewidth of the TCPS for the CTP configuration evidently narrower than that for the CP configuration. A TCPS with spectral linewidth ~4.2 MHz in the CTP configuration is obtained in the experiment, which is near the natural linewidth $(\Gamma_2 + \Gamma_3)/2 = (5.2 + 2.2)/2 = 3.7$ MHz of the $6P_{3/2}\,F' = 5 - 8S_{1/2}\,F'' = 4$ transition. Finally, an optimized TCPS as the error signal at the pump power ~1.0 mW is fed back into the PZT port of the 794.6 nm laser by a PID module for frequency stabilization without frequency modulation, and the residual frequency fluctuation after locking on is estimated at ~0.9 MHz within 400 s. This technique of locking frequency can be applied to the two-color (852.3 nm + 794.6 nm) magneto-optical trap experiment in future[8,9].

This work was financially supported by the National Natural Science Foundation of China (Nos. 11774210, 11104172, and 61575112) and the National Key Research and Development Program of China (No. 2017YFA0304502).

References

1. J. Wang, H. F. Liu, G. Yang, B. D. Yang, and J. M. Wang, Phys. Rev. A **90**, 052505 (2014).
2. Y. N. Ren, B. D. Yang, J. Wang, G. Yang, and J. M. Wang, Acta Phys. Sin. **65**, 073103 (2016).
3. A. K. Mohapatra, T. R. Jackson, and C. S. Adams, Phys. Rev. Lett. **98**, 113003 (2007).
4. S. C. Bell, D. M. Heywood, J. D. White, J. D. Close, and R. E. Scholten, Appl. Phys. Lett. **90**, 171120 (2007).
5. P. Y. Chang, T. T. Shi, S. N. Zhang, H. S. Shang, D. Pan, and J. B. Chen, Chin. Opt. Lett. **15**, 121401 (2017).
6. R. T. Willis, F. E. Becerra, L. A. Orozco, and S. L. Rolston, Phys. Rev. A **79**, 033814 (2009).
7. S. J. Wu, T. Plisson, R. C. Brown, W. D. Phillips, and J. V. Porto, Phys. Rev. Lett. **103**, 173003 (2009).
8. B. D. Yang, Q. B. Liang, J. He, and J. M. Wang, Opt. Express **20**, 11944 (2012).
9. B. D. Yang, J. Wang, and J. M. Wang, Chin. Opt. Lett. **14**, 040201 (2016).
10. J. Wang, G. Yang, J. He, and J. M. Wang, Chin. Opt. Lett. **15**, 050203 (2017).
11. R. Boucher, M. Breton, N. Cyr, C. Julien, and M. Tetu, IEEE Photonics Technol. Lett. **4**, 327 (1992).
12. H. S. Moon, W. K. Lee, L. Lee, and J. B. Kim, Appl. Phys. Lett. **85**, 3965 (2004).

13. B. D. Yang, J. Y. Zhao, T. C. Zhang, and J. M. Wang, J. Phys. D **42**, 085111 (2009).
14. C. Carr, C. S. Adams, and K. J. Weatherill, Opt. Lett. **37**, 118 (2012).
15. H. R. Noh, Opt. Express **20**, 21784 (2012).
16. B. D. Yang, J. Wang, H. F. Liu, J. He, and J. M. Wang, Opt. Commun. **319**, 174 (2014).
17. P. Kulatunga, H. C. Busch, L. R. Andrews, and C. I. Sukenik, Opt. Commun. **285**, 2851 (2012).
18. X. H. Fu, K. K. Liu, R. C. Zhao, W. Gou, J. F. Sun, Z. Xu, and Y. Z. Wang, Chin. Opt. Lett. **13**, 073001 (2015).
19. B. D. Yang, J. Gao, T. C. Zhang, and J. M. Wang, Phys. Rev. A **83**, 013818 (2011).
20. J. Gea-Banacloche, Y. Q. Li, S. Z. Jin, and M. Xiao, Phys. Rev. A **51**, 576 (1995).
21. Y. Lee and H. S. Moon, Opt. Express **24**, 10723 (2016).